Microcirculation, 14: 125–136, 2007

ISSN: 1073-9688 print / 1549-8719 online
DOI: 10.1080/10739680601131218

informa
healthcare

Abrupt Reoxygenation of Microvascular Endothelial Cells After Hypoxia Activates ERK1/2 and JNK1, Leading to NADPH Oxidase-Dependent Oxidant Production

GUO YU,[*,‡] TIANQING PENG,[*,§] QINGPING FENG,[*,†,§] AND KAREL TYML[*,†,‡]
[*]The Centre for Critical Illness Research, Lawson Health Research Institute, and Departments of [†]Physiology and Pharmacology, [‡]Medical Biophysics, and [§]Medicine, University of Western Ontario, London, Canada

ABSTRACT

Objective: Mitogen-activated protein kinases (MAPK) in microvascular endothelial cells (EC) may participate in organ pathophysiology following hypoxia/reoxygenation (H/R). The authors aimed to determine the role of MAPK in H/R-induced reactive oxygen species (ROS) generation in mouse microvascular EC.

Methods: Cultured EC derived from skeletal muscle of male wild-type (WT), gp91phox$^{-/-}$ or p47phox$^{-/-}$ mice were subjected to hypoxia (0.1% O_2, 1 h) followed by abrupt reoxygenation, H/R_A (hypoxic medium quickly replaced by normoxic medium), or slow reoxygenation, H/R_S (O_2 diffused to cells through hypoxic medium). Cells were analyzed for ERK, JNK, and p38 MAPK phosphorylation, NADPH oxidase activation, and ROS generation.

Results: In WT cells, H/R_A but not H/R_S rapidly phosphorylated ERK1/2 and JNK1 and subsequently increased ROS production. H/R_A did not affect p38. MAPK phosphorylation persisted despite inhibition of NADPH oxidase, mitochondrial respiration, protein tyrosine kinase, or PKC. ROS increase during H/R_A was prevented by deletion of gp91phox or p47phox, or MAPK inhibition.

Conclusions: Abrupt reoxygenation after hypoxia activates ERK1/2 and JNK1 in mouse microvascular endothelial cells via a tyrosine kinase-, PKC-, and NADPH oxidase-insensitive mechanism, leading to increased NADPH oxidase-dependent ROS production. The results suggest that MAPK activation in the microvascular endothelium is O_2-sensitive, contributing critically to tissue pathophysiology after H/R.
Microcirculation (2007) **14,** 125–136. doi:10.1080/10739680601131218

KEY WORDS: MAP kinases, microvascular endothelium, oxidative stress

Hypoxia and reoxygenation (H/R) is a key component of the complex pathophysiology of ischemia and reperfusion in a given organ. In the cardiovascular system, there is substantial evidence that H/R alters cellular function via activation of a family of mitogen-activated protein kinases (MAPK) [20, 25]. The family includes 3 distinct terminal kinases: the extracellular signal-regulated kinase (ERK), c-Jun NH2-terminal kinase (JNK), and p38 MAPK [20]. H/R-activated MAP kinases can precipitate long-term effects (e.g., altered expression of proteins, cell proliferation) [25, 28] as well as rapid events such as modulation of cell-to-cell coupling [26]. Recently, we reported that H/R reduces interendothelial cell coupling and phosphorylates ERK1/2 as early as 4 min after reoxygenation. MEK1/2 inhibition prevented both the H/R-induced MAPK phosphorylation and reduced coupling [26].

The mechanism of MAPK activation by H/R is poorly understood. Generally, NADPH oxidase activation and subsequent reactive oxygen species (ROS) generation shortly after reoxygenation [13] have been shown to initiate MAPK signaling [4, 6, 20]. However, ROS did not initiate p38 MAPK

We thank M. Bolon, F. Wu, M. Keet, and S. Lu for technical assistance. The work was supported by grants from the Canadian Institutes of Health Research (MOP 53342), and the Heart and Stroke Foundation of Ontario (NA 5568) (awarded to K.T.).

Address correspondence to K. Tyml, PhD, Victoria Research Laboratory, 6th Floor, 800 Commissioners Road East, London, Canada N6C 2V5. E-mail: ktyml@lhsc.on.ca

Received 4 May 2006; accepted 23 August 2006.

phosphorylation in mouse cardiac fibroblasts [27], while inhibition of p38 and MEK1/2 attenuated hyperoxia-induced, NADPH oxidase-dependent ROS production in human lung endothelial cells [24], suggesting that MAPK signaling could also be upstream of NADPH oxidase.

Evidence for ROS initiation in MAPK signaling in the vasculature comes from studies using cells derived from large blood vessels [10]. Yet, during the clinical condition of ischemia/reperfusion (e.g., myocardial infarction), it is the smallest blood vessels downstream from occlusion that are exposed to H/R. The microvascular endothelium, in particular, may critically participate in the development of pathophysiology after H/R [12, 16], including altered minute-to-minute regulation of blood flow in the reoxygenation phase where the rate of reoxygenation could dictate the degree of reperfusion-related tissue injury [14, 18].

To our knowledge, the effect of H/R on rapid MAPK signaling and the role of ROS in this signaling have not been examined in microvascular endothelial cells. The main objective of the present study was to determine this effect in mouse microvascular endothelial cells (MMEC) derived from skeletal muscle. The rationale for using these cells was our recent report that abrupt but not slow reoxygenation of MMEC rapidly reduces intercellular electrical coupling [2], via a MAPK-sensitive mechanism [26]. The present study shows for the first time that abrupt, but not slow reoxygenation activates ERK1/2 and JNK1 in MMEC within several minutes of reoxygenation, leading to a large, NADPH oxidase-dependent increase in ROS production in these cells. Because of the importance of microvascular endothelium in blood flow control and the attendant oxygen delivery to the tissue during the reoxygenation phase, rapid MAPK signaling during this phase could critically contribute to the development of tissue pathophysiology after H/R.

MATERIALS AND METHODS

Reagents

Rabbit monoclonal anti-phospho-ERK1/2 and anti-ERK1/2, anti-phospho-JNK1/2, anti-JNK1/2, anti-phospho-p38MAPK, and anti-p38MAPK antibodies were purchased from Cell Signaling Technology (Beverly, MA). Peroxidase-labeled anti-rabbit IgG was included in the primary antibody kit. SiRNA for ERK1 and ERK2 were from Santa Cruz Biotechnology (Santa Cruz, CA). An adenoviral vector containing a dominant negative mutant of JNK1 (ad-dnJNK1) was obtained from K. Webster (University of Miami School of Medicine), while adenoviral vector containing green fluorescence protein (ad-GFP) was obtained from J. Lipp (Medical University of Vienna). MEK1/2 inhibitor U0126, JNK inhibitor SP600165, protein tyrosine kinase inhibitors genistein and PP-2, and PKC inhibitor bisindolylmaleimide 1 were obtained from Calbiochem (La Jolla, CA). The antioxidants L-ascorbic acid and superoxide dismutase-polyethylene glycol (PEG-SOD), NADPH oxidase inhibitors apocynin and diphenyleneiodonium (DPI), mitochondrial respiration blocker rotenone, nitric oxide synthase inhibitor L-NAME hydrochloride, xanthine oxidase inhibitor allopurinol, nitro blue tetrazolium (NBT), Griffonia simplicifolia-I (GS-I) lectin, dispase, trypsin, bovine serum albumin (BSA), collagenase II, dimethysulfoxide (DMSO), DMEM/F12, fetal bovine serum (FBS), dialyzed FBS, protease inhibitor cocktail (catalog # P2714), phosphotase inhibitor mix (catalog # P5726), and Dulbecco phosphate-buffered saline (PBS) were all purchased from Sigma Chemical (St. Louis, MO). Endothelial growth supplement and anti-GAPDH antibody were from BD Biosciences (Mississauga, ON). Magnetic beads and magnetic particle concentrator were purchased from Dynal (Lake Success, NY). Heparin was from Leo Laboratories (Ajax, ON). DMEM/HEPES, L-glutamine, antibiotic-antimycotic solution, and Triazol reagent were from Gibco (Mississauga, ON).

Cell Isolation and Culture

Animals were handled in accordance with the guidelines of the Canadian Council on Animal Care. Protocols were approved by the Animal Use Subcommittee at the University of Western Ontario. We used male C57BL/6 wild-type, gp91phox$^{-/-}$ and p47 phox$^{-/-}$ mice at the age of 6–8 weeks (Jackson Laboratories, Bar Harbor, ME) (gp91phox and p47phox are subunits of NADPH oxidase). Mouse microvascular endothelial cells were harvested from the hindlimb muscle, as described previously [21]. Briefly, the muscle was excised, minced, and digested in an enzyme solution. The digest was filtered through a nylon mesh and cells were collected and washed in DMEM/F12. Cells were grown to confluence and then purified by immunoseparation using GS-I lectin coated magnetic beads. MMEC were then cultured in maintenance medium containing DMEM/F12, FBS (10%), endothelial growth supplement (100 μg/mL), heparin (5 U/mL), L-glutamine (0.2 mM), and antibiotic-antimycotic

solution (10 μg/mL) in standard incubator normoxic conditions (5% CO_2, 19% O_2, and 76% N_2 at 37°C). Cells were used between passages 4 and 12. Endothelial phenotype was determined by the presence of von Willebrand factor and GS-I lectin antigens as detailed by us [34]. Thirty or sixty minutes prior to experiments, the maintenance medium was replaced by a dialyzed serum medium (DSM, 5% dialyzed serum in DMEM/F12, without endothelial growth supplement and glutamine). Selected doses of agents used in experiments were based on the literature and/or positive control experiments carried out in our laboratory.

Exposure of Cells to Hypoxia, and Abrupt or Slow Reoxygenation

Hypoxic DSM was prepared by bubbling DSM with 100% N_2 for 5 min prior to experiments. Cells were covered by a 1.2-mm-thick layer of hypoxic DSM and then placed into a hypoxic incubator (5% CO_2, 0.1% O_2 and 94.9% N_2 at 37°C). After 1 h of hypoxia (duration in all experiments), cells were subjected either to abrupt (H/R_A) or slow reoxygenation (H/R_S). The rationale for these 2 protocols was the concept that hypoxic reperfusion attenuates postischemic microvascular injury [18], suggesting that the rate of reoxygenation after hypoxia plays a role in this injury [14]. For abrupt reoxygenation, hypoxic DSM was replaced (within several seconds) by prewarmed and pH-equilibrated normoxic DSM and cells were placed into the standard normoxic incubator for specified time. Normoxic DSM was either fresh (DSM was kept in normoxic incubator for at least 1 h) or "conditioned" by cells during hypoxia (hypoxic DSM collected from separate cells after 1 h hypoxia was reequilibrated with oxygen in normoxic incubator for at least 1 h). For slow reoxygenation, cells were left covered in the hypoxic medium and, without stirring, placed into the normoxic incubator. Oxygen here diffused to the cells through the 1.2-mm layer of hypoxic medium, resulting in a slower reoxygenation than that of the H/R_A protocol. Using a PO_2 microsensor (OxyLite, Oxford Optronix, UK), we observed that the hypoxic medium gradually recovered to complete normoxia in ~10 min (50% recovery to normoxia occurred in ~3 min). Control cells for the H/R_A protocol were kept in normoxic incubator. They were exposed for 1 h to normoxic DSM, which was then replaced by fresh normoxic DSM (cells experienced the same shear stress caused by replacing DSM as cells in H/R_A protocol). "Shear stress" controls for the H/R_S protocol included pipetting hypoxic DSM out and back into the culture dish, and then placing the dish in the hypoxic incubator.

Transfection with siRNA and Adenoviral Infection

For ERK1 and ERK2 siRNA transfection, cells were cultured in 24-well plate to 70–80% confluency. Transfection was done according to manufacturer's instructions (Qiagen). Eight microliters of siRNA (10 μM) was applied to each well for 3 h (final concentration of siRNA was 0.3 μM). After transfection, cells were kept in the maintenance medium for another 48 h, after which cells in parallel wells were used either for the total protein measurement or for studying the effect of H/R_A on ROS production. Ad-dnJNK1 was applied to 80–90% confluent cells in the maintenance medium at a multiplicity of infection 100 pfu/cell for 1 h and then cells were cultured for another 48 h to study the effect of H/R_A on ROS production. Ad-GFP was used as a negative control (at the same concentration as ad-dnJNK1).

Western Blots

Cells were washed, lysed, and proteins denatured and centrifuged as reported by us [21]. The supernatant was stored at −20°C. Protein amount was quantified using the Bio-Rad DC Protein Assay (BioRad, Hercules, CA). Absorbances were read on Beckman microplate reader (BioRad, model 3550-UV). Equal amounts of protein (10 μg for ERK and 30 μg for JNK analyses) were fractionated on SDS/polyacrylamide gel (10%) and electrotransferred to polyvinylidene difluoride microporous membrane (Millipore, Bedford, MA) using a semi-dry system (BioRad). Membranes were blocked with 5% nonfat milk in Tris–buffer saline containing 0.05% tween-20 for 1 h at room temperature or overnight at 4°C, and then incubated with specific antibodies (1:1000) for 1–2 h. After washing, the blots were incubated with a 1:2500 dilution of anti-rabbit IgG peroxidase-conjugated antibody for 1 h. The bands were visualized using an enhanced chemiluminescence (ECL) detection system (Cell Signaling, Beverly, MA) with Kodak BioMax MR imaging film (Rochester, NY). To reprobe membranes, we stripped them with a buffer containing Tris–HCl (62.5 mM, pH 6.7), 2% SDS and 2-mercaptoethanol (100 mM) at 55°C for 30 min. The results of phospho- and nonphosphorylated ERK1/2 and phospho- and nonphosphorylated JNK1/2 came from the same membrane.

Measurement of ROS Production

Nitroblue tetrazolium (NBT) assay was used to measure intracellular ROS [36]. MMEC were seeded with

equal density on 24-well plates to reach confluence. NBT was completely dissolved in DSM (rather than in DMSO) at 37°C. Cell culture medium was replaced with DSM containing 1 mg/mL of NBT for 30 min before the onset of hypoxia. Some experiments were performed in the presence of L-NAME, allopurinol, DPI, PEG-SOD, U0126, or SP600125 applied 30 min prior and during H/R_A. After the experiment, cells were rinsed with 2 M NaOH, and formazan was dissolved in 1 mL of DMSO. Optical density was measured at 654 nm with DU 640 spectrophotometer (Beckman, Fullerton, CA). Since formazan prevented protein quantification measurement in the same well, cells in parallel wells were used for this purpose. To verify that all wells per plate had the same cell confluence/total protein, we measured protein amount in some of these wells selected at random (outcome: no more than 5% difference in protein/well was seen). To confirm ROS production in MMEC, we also used the dihydrorhodamine 123 (DHR 123) assay as detailed in our previous report [35].

Measurement of NADPH Oxidase Activity

Cells were cultured in 6-well plates to confluence. Culture medium was replaced with DSM containing U0126 or SP600125 for 30 min before H/R_A (agents continued to be present during H/R_A). Cells were washed twice with ice-cold PBS containing 0.1% BSA, and then were collected by scraping in 0.6 mL DMEM/HEPES buffer containing 100× diluted protease inhibitor cocktail (as suggested by the manufacturer) and MAPK inhibitors. The samples were homogenized by sonication for 5 s (setting 25, Ultrasonic Homogenizer model 4710, Cole Parmer, Chicago, IL) and incubated on ice for 20 min for further NADPH oxidase activity analysis. The activity was measured using a modified lucigenin chemiluminescence assay [22]. Briefly, 10 μL of NADPH (100 μM) was added to 100 μL of sample on 96-well plate (white wells in black matrix). After keeping the mixture for 10 min at 37°C, 5 μM lucigenin (final concentration) was added, and NADPH-dependent superoxide generation was immediately measured every 5 s for 12 min using a multilabel Perkin Elmer Wallac Victor 3 counter. We used the average count/second (cps) per 100 μg of protein as a measure of NADPH oxidase activity.

Statistics

Data are presented as means ± SE (n is the number of independent experiments/treatment group) and are based on MMEC isolated from at least 3 different mice. We used analysis of variance followed by Student's t test with Bonferroni correction for multiple comparisons at significance $p < .05$.

RESULTS

H/R_A but Not H/R_S Rapidly Activates ERK1/2 and JNK1

To assess the role of reoxygenation in H/R-initiated MAPK signaling, MMEC were exposed to hypoxia alone, or to hypoxia followed by abrupt or slow reoxygenation. Figure 1A and B shows no activation of ERK or JNK at the end of 1 h hypoxia (lane 2). Abrupt reoxygenation (fresh normoxic DSM) markedly increased phosphorylation of ERK1/2 and JNK1 (lanes 3 and 4), which returned to control in 30 min (lane 5). Abrupt reoxygenation using the "conditioned" DSM comparably phosphorylated ERK1/2 and JNK1 (lane 9). By contrast, slow reoxygenation caused no phosphorylation within the 30-min period (lanes 6-8). Shear stress controls for H/R_A and H/R_S yielded negligible phosphorylation (lanes 1 and 10, respectively). Neither hypoxia alone nor abrupt reoxygenation phosphorylated p38 MAPK within 30 min (data not shown). Figure 1C and D shows that H/R_A-induced phosphorylation of ERK1/2 and JNK1 were inhibited by U0126 and SP600125, respectively.

MAPK Activation by H/R_A Is gp91phox- and ROS-Insensitive

To examine a possible role of NADPH oxidase in initiating H/R_A-induced MAPK signaling [4], we probed for phosphorylated ERK1/2 and JNK1 in gp91phox $^{-/-}$ MMEC. Figure 2A and B demonstrates that gp91phox deletion did not affect ERK1/2 and JNK1 phosphorylation. Consistently, Figure 2C and D shows that neither the NADPH oxidase inhibitor DPI nor antioxidant PEG-SOD affected the H/R_A-induced ERK1/2 and JNK1 phosphorylation. To further probe into MAPK activation by H/R_A, we examined the effect of apocynin (an alternative NADPH oxidase inhibitor) and rotenone (mitochondrial respiration blocker) on ERK1/2 and JNK1 phosphorylation. None of these agents affected this phosphorylation (Figure 3). Consistent with these results, preloading MMEC with the antioxidant ascorbate (100 μM over 24 h) [35] had no effect on H/R_A-induced ERK1/2 and JNK1 phosphorylation (data not shown).

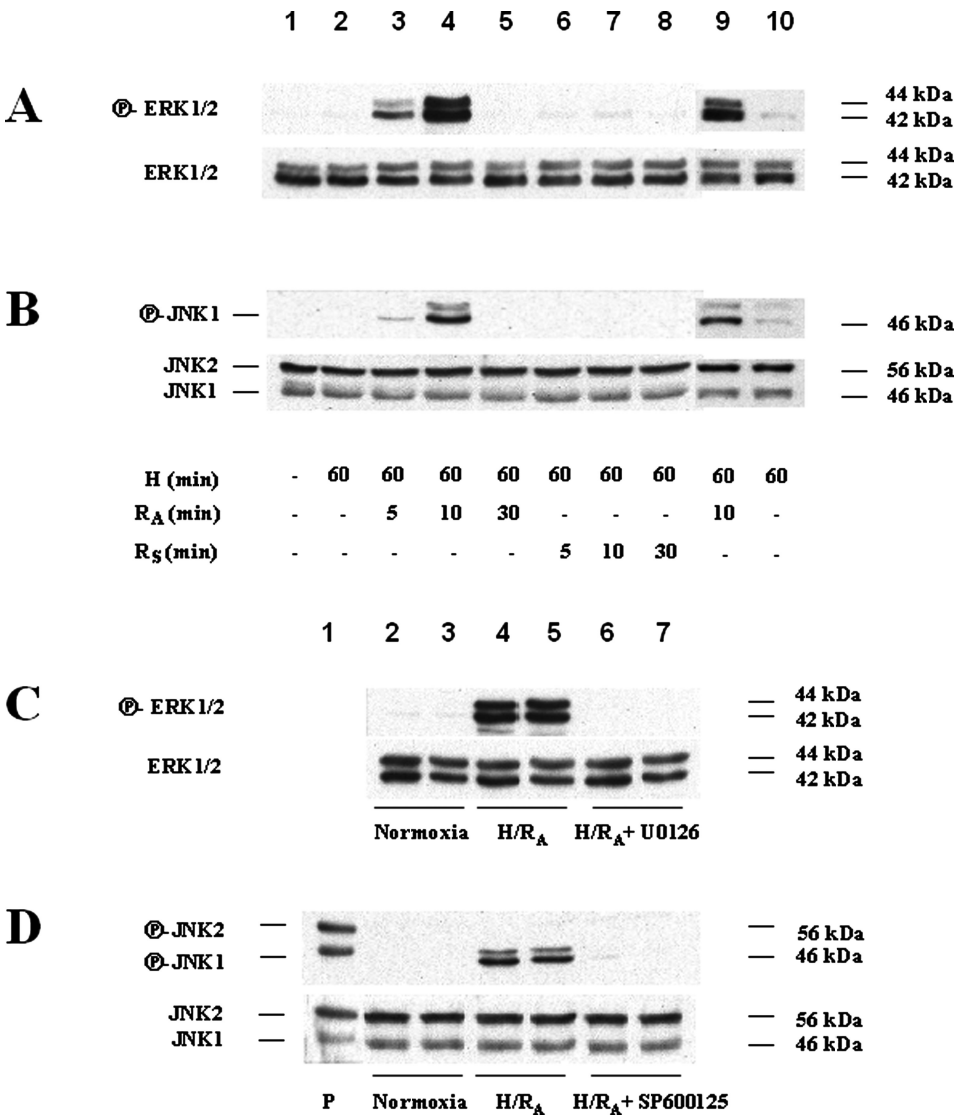

Figure 1. Abrupt but not slow reoxygenation after hypoxia increases MAP kinase phosphorylation. Monolayers of cultured microvascular endothelial cells (MMEC) harvested from skeletal muscle of male wild-type (WT) mice were subjected to hypoxia (H; 0.1% O_2, 1 h) followed either by abrupt reoxygenation (R_A; hypoxic medium quickly replaced by fresh normoxic medium), or by slow reoxygenation (R_S; O_2 diffused to cells through 1.2 mm unstirred hypoxic culture medium). (A, B) Examples of western blots of phosphorylated and nonphosphorylated ERK, and of phosphorylated JNK and nonphosphorylated JNK, after hypoxia and increasing times of abrupt (lanes 3–5) or slow reoxygenation (lanes 6–8), respectively. When cells were reoxygenated with normoxic medium previously "preconditioned" by hypoxic cells, phosphorylation of ERK1/2 and JNK1 was also observed (lane 9). MAPK activation was not due to a possible shear stress effect (33) associated with replacement of culture medium, since replacing medium only, either in normoxic cells or in hypoxic cells without subsequent reoxygenation, did not cause MAPK phosphorylation (lanes 1 and 10, respectively). Shown are representative examples of 3 blots per group. (C) MMEC from WT mice were treated with MEK1/2 inhibitor U0126 (20 μM, lanes 6, 7) or vehicle (lanes 4, 5) for 30 min prior to hypoxia, during hypoxia (1 h), and during reoxygenation (10 min). U0126 inhibited the H/R_A-induced ERK1/2 phosphorylation (lanes 6, 7 vs. lanes 4, 5). (D) Wild-type MMEC were treated with JNK inhibitor SP600125 (20 μM, lanes 6, 7) or vehicle (lanes 4, 5) for 30 min prior to hypoxia and during H/R_A. SP600125 inhibited H/R_A-induced JNK1 phosphorylation (lanes 6, 7 vs. lanes 4, 5). Lane 1 shows blots of phosphorylated JNK1/2 and nonphosphorylated JNK1/2 from UV treated 293 cell line provided by the antibody manufacturer as positive control (P). Since phospho-JNK2 band in lane 1 migrated slower than the upper band of phospho-JNK1 blot in lanes 4, 5, we interpret this upper band to represent an isoform of JNK1 (3). Cells in lanes 2, 3 (C and D) were subjected to control normoxic conditions. C and D show western blots from two independent experiments (MMEC originated from two WT mice), in lanes 3, 5 and 7 (Exp. 1) and in lanes 2, 4, and 6 (Exp. 2).

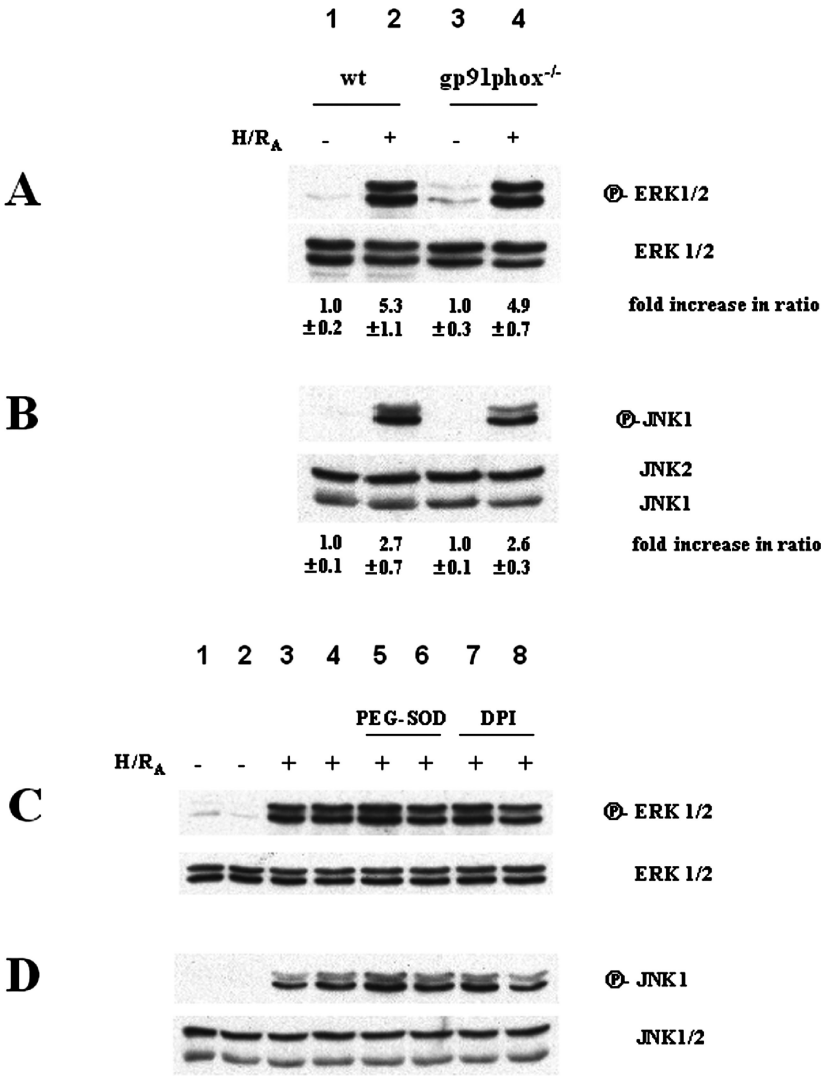

Figure 2. H/R_A-induced MAPK phosphorylation is gp91phox-insensitive. (A, B) Examples of western blots of phosphorylated and nonphosphorylated ERK and JNK in WT and gp91phox$^{-/-}$ cells subjected to normoxia or H/R_A (10 min). Shown also are fold increases in density ratio between phospho-ERK1/2 and ERK1/2 blots and between phospho-JNK1 and JNK1 blots, normalized to respective controls (lanes 1, 3). There was no difference in MAPK activation between WT and gp91phox$^{-/-}$ groups subjected to H/R_A (lane 4 vs. 2). Shown are representative examples of 3 blots per group. (C, D) Examples of western blots of phosphorylated and nonphosphorylated ERK and JNK in WT cells subjected to normoxia or H/R_A (10 min), with and without treatment with the antioxidant superoxide dismutase-polyethylene glycol (PEG-SOD, 100 U/mL) or NADPH oxidase inhibitor diphenyleneiodonium (DPI, 10 μM). Agents were applied 30 min prior and during H/R_A. There was no effect of PEG-SOD or DPI on H/R_A-induced EKR1/2 or JNK1 phosphorylation. From the total of 3 independent experiments, shown are 2 independent experiments in lanes 1, 3, 5, and 7 (Exp. 1) and in lanes 2, 4, 6, and 8 (Exp. 2).

Effect of Protein Tyrosine Kinase and PKC Inhibition on MAPK Activation

Since activated c-Src and PKC appear to be upstream signaling events leading to ERK1/2 phosphorylation [4, 30], we tested whether H/R_A-induced ERK1/2 or JNK1 phosphorylation is tyrosine kinase and PKC-sensitive. Figure 4 shows that neither c-Src inhibitor PP-2 nor PKC inhibitor bisindolylmaleimide 1 affected this phosphorylation. Consistently, the tyrosine kinase inhibitor genistein (20 μM) also had no effect on this phosphorylation (data not shown).

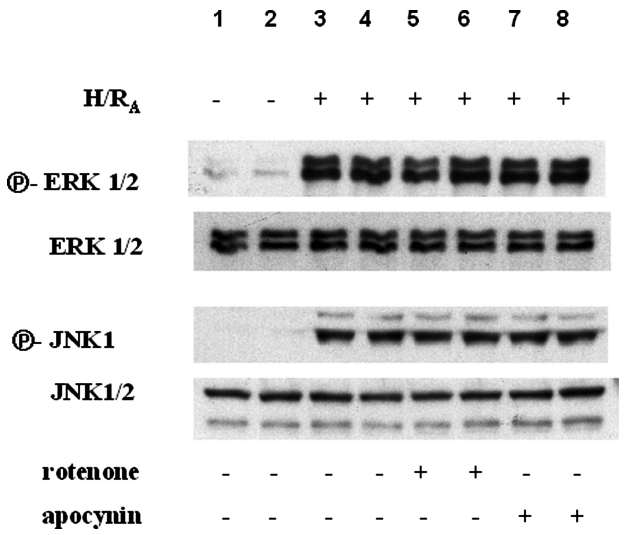

Figure 3. Effect of NADPH oxidase inhibitor apocynin and mitochondrial respiration blocker rotenone on H/R$_A$-induced ERK1/2 and JNK1 phosphorylation in wild-type MMEC. Cells were exposed to normoxia (lanes 1 and 2) or H/R$_A$ (10 min) (lanes 3–8), with or without treatment with apocynin (1 mM) or rotenone (10 μM). Agents were applied 1 h prior and during H/R$_A$. Based on 3 independent experiments, neither agent affected H/R$_A$-induced ERK1/2 and JNK1 phosphorylation. Shown are Western blots from two of these experiments in lanes 1, 3, 5, and 7 (Exp. 1) and in lanes 2, 4, 6, and 8 (Exp. 2).

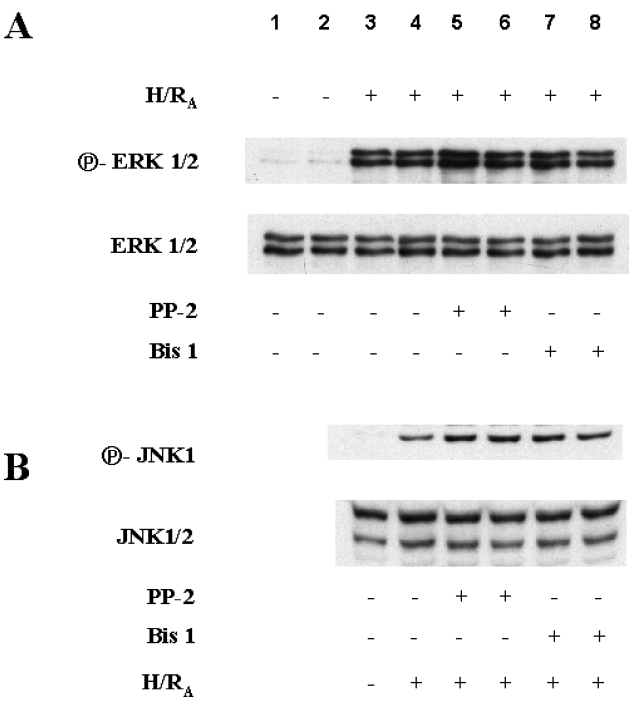

Figure 4. Effect of protein tyrosine kinase or PKC inhibition on ERK1/2 and JNK1 phosphorylation in wild-type MMEC. Cells were exposed to normoxia (lanes 1 and 2 in (A); lane 3 in (B)) or H/R$_A$ (10 min) (lanes 3–8 in (A); lanes 4–8 in (B)), with or without treatment with c-Src inhibitor PP-2 (10 nM), or PKC inhibitor bisindolylmaleimide 1 (Bis 1, 500 nM). Agents were applied 1 h prior and during H/R$_A$. Based on 3 independent experiments, neither agent affected H/R$_A$-induced ERK1/2 phosphorylation. (A) Western blots from two of these experiments in lanes 1, 3, 5, and 7 (Exp. 1) and in lanes 2, 4, 6, and 8 (Exp. 2). (B) Western blots from one of these experiments in lanes 3, 4, 5, and 7 (lanes 6 and 8 are duplicates of lanes 5 and 7, respectively).

Effect of H/R$_A$ and H/R$_S$ on ROS Production

One hour hypoxia alone caused a slight but statistically insignificant increase in intracellular ROS level (Figure 5A, bar 2). Abrupt reoxygenation increased this level by ~100% (i.e., at 30–60 min of reoxygenation; Figure 5A, bars 5 and 6), which subsequently returned to control in 180 min (Figure 5A, bar 8). Figure 5B confirms this increase using the DHR 123 assay. By contrast, slow reoxygenation increased ROS level slightly by ~30% at 30 min of reoxygenation (Figure 5A, bar 9), not beyond the level of hypoxia alone. The baseline ROS during normoxia could partly be produced by endothelial NADPH oxidase, as lowered baseline was found in MMEC derived from gp91phox$^{-/-}$ or p47phox$^{-/-}$ mice (Figure 6A, bars 5 and 7). However, the H/R$_A$-induced ROS increase originated entirely from endothelial NADPH oxidase, as H/R$_A$ did not elevate ROS in cells from gp91phox$^{-/-}$ or p47phox$^{-/-}$ mice (Figure 6A, bars 5–8). Consistently, both DPI and PEG-SOD reduced baseline ROS, and attenuated H/R$_A$-induced ROS increase (Figure 6B), while inhibition of XO with allopurinol and inhibition of NOS with L-NAME (other potential sources of ROS) did not prevent the H/R$_A$-induced ROS increase (Figure 6A, bars 3 and 4).

Inhibition of MAPK Activation Prevents H/R$_A$-Induced ROS Increase

Figure 7A demonstrates that, based on the NBT assay, the MEK1/2 inhibitor U0126 attenuated and the JNK inhibitor SP600125 completely prevented the H/R$_A$-induced increase in ROS. Figure 8B and C confirms these results using inhibition of ERK1/2 with the appropriate siRNA and inhibition of JNK1 with ad-dnJNK1, respectively. (Application of ERK1 siRNA and ERK2 siRNA inhibited ERK1 and ERK2 protein expression, respectively (Figure 8A), while application of ad-dnJNK1 inhibited H/R$_A$-induced

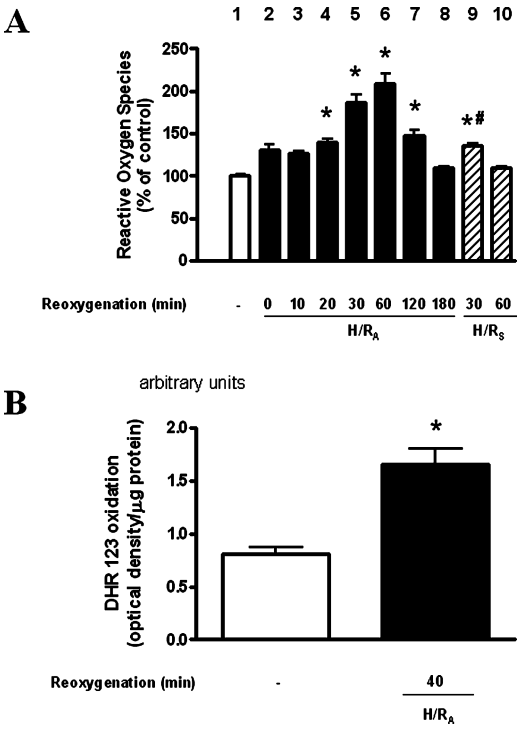

Figure 5. Effect of H/R_A and H/R_S on reactive oxygen species (ROS) production in wild-type MMEC. (A) Cells were exposed to normoxia or hypoxia for 1 h, and then subjected to abrupt or slow reoxygenation for increasing duration as shown. H/R_A markedly increased ROS at 30–60 min of reoxygenation (ROS measured by NBT assay; details under Methods). *Difference from control (bar 1), #difference between time-matched responses to H/R_A and H/R_S (bar 9 vs. 5), $p < .05$, $n = 5$–10. (B) Confirmation of H/R_A-induced ROS, using the dihydrorhodamine 123 (DHR 123) assay (35). *Difference from control (left bar), $p < .05$, $n = 9$.

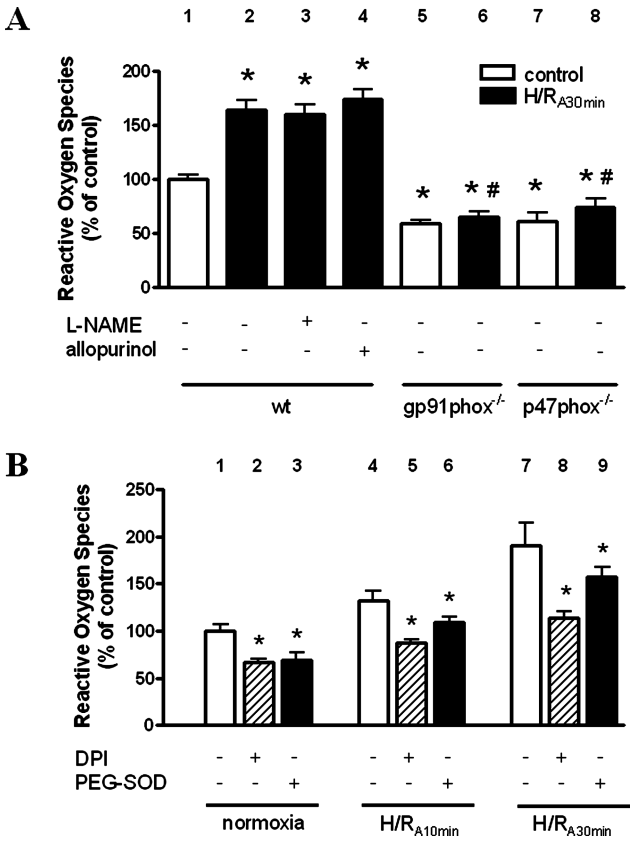

Figure 6. H/R_A-induced ROS production in MMEC is NADPH oxidase-dependent. (A) Cells from WT, gp91phox$^{-/-}$ and p47 phox$^{-/-}$ mice were seeded with equal density on 24-well plates to reach consistent confluency at 1×10^5 cells/well. Consistence was verified by measuring protein amount in some of these wells selected at random. H/R_A-induced ROS in WT cells (bar 2 vs. 1) was absent in cells from gp91phox$^{-/-}$ and p47phox$^{-/-}$ mice (bars 6 vs. 5 and 8 vs. 7). NOS inhibitor L-NAME (1 mM, bar 3) or XO inhibitor allopurinol (100 μM, bar 4) had no effect on H/R_A-induced ROS. *Difference from control (bar 1), #difference from H/R_A group in WT cells (bar 2), $p < .05$, $n = 6$–10. (B) Production of ROS in WT cells, normalized with respect to untreated normoxic cells (bar 1). DPI (10 μM) or PEG-SOD (50 μM) inhibited ROS production in cells during normoxia and after H/R_A. *Difference from controls (bars 1, 4 and 7) in the normoxia, H/R_{A10min} and H/R_{A30min} groups, respectively. $p < .05$, $n = 5$–8.

phosphorylation of JNK1 (data not shown)). Based on the lucigenin assay, Figure 7B shows that both pharmacological inhibitors prevented the H/R_A-induced NADPH-dependent superoxide generation. Together, Figures 7 and 8 indicate that the H/R_A-induced, NADPH oxidase-mediated ROS increase was MAPK-dependent.

Regarding the more potent inhibitory effect of SP600125 versus U0126 on ROS/superoxide production (Figure 7A and B, bars 5 and 6), it is possible that JNK could be a more important component of H/R_A-induced signaling than ERK. However, it is also possible that SP600125 at 20 μM concentration partially inhibited ERK activation [1]. To this end, we found that SP600125 dose-dependently inhibited H/R_A-induced superoxide production (Figure 7C), suggesting a minimal effect of SP600125 on ERK-dependent superoxide production. A direct testing of the partial inhibition of ERK activation, requiring biochemical characterization of ERK enzyme activity in the presence of SP600125 [1], was beyond the scope of the present study.

DISCUSSION

To our knowledge, we show for the first time in mouse microvascular endothelial cells that abrupt, but not slow reoxygenation following hypoxia rapidly

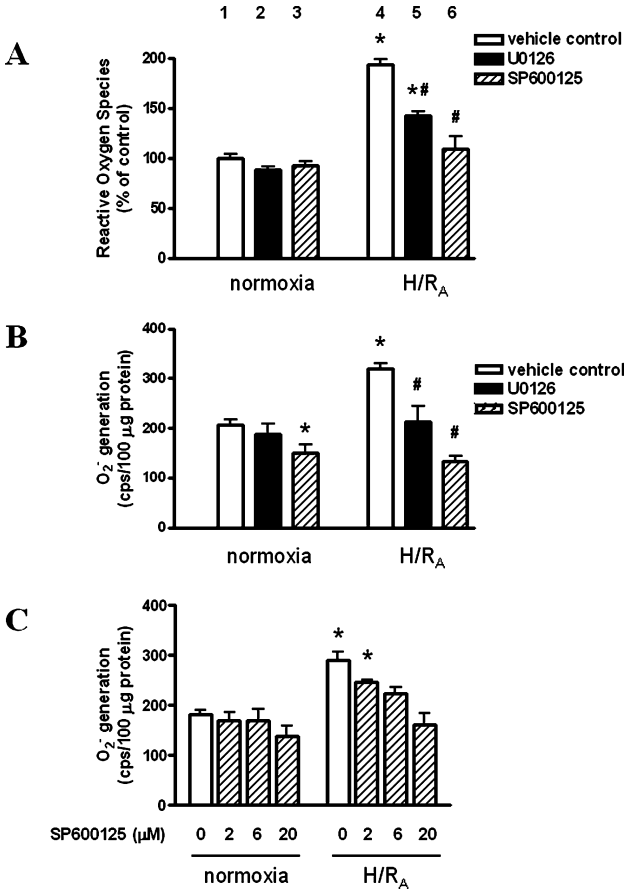

Figure 7. Pharmacological inhibition of MAPK prevents ROS and $O_2^{\bullet -}$ generation induced by H/R_A. (A) WT cells were treated with U0126 (20 μM), SP600125 (20 μM), or vehicle (control group) for 30 min, and then subjected to H/R_A (30 min) or normoxia (agents continued to be present during H/R_A or normoxia). ROS production was determined by NBT assay and normalized to the vehicle-treated group subjected to normoxia. *Difference from bar 1, #difference from bar 4, $p < .05$, $n = 4$–6. (B) WT cells were treated with U0126 (20 μM), SP600125 (20 μM), or vehicle 30 min prior and during H/R_A (40 min) or normoxia. NADPH-dependent $O_2^{\bullet -}$ generation in cells was determined by the lucigenin chemiluminescence assay. *Difference from bar 1, #difference from bar 4, $p < .05$, $n = 4$–6. (C) WT cells were treated with SP600125 (0 to 20 μM) 30 min prior and during H/R_A (40 min) or normoxia. NADPH-dependent $O_2^{\bullet -}$ generation in cells was determined by the lucigenin chemiluminescence assay. *Difference from normoxic group at 0 μM SP600125, $p < .05$, $n = 3$–5.

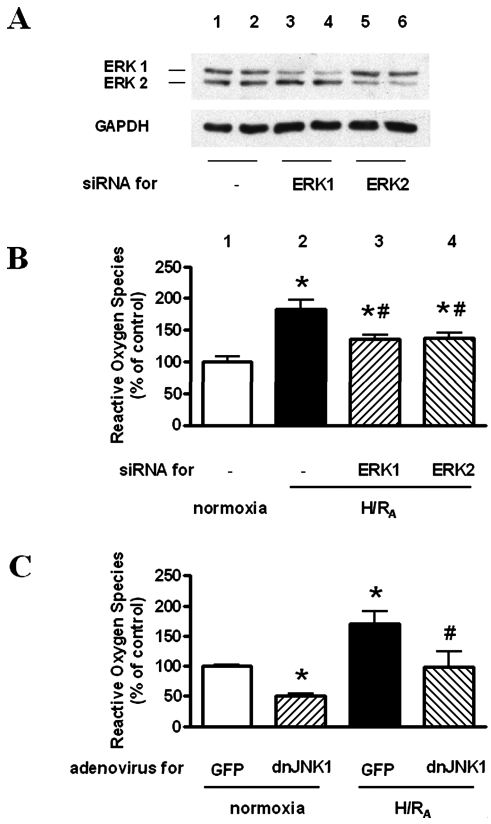

Figure 8. Knock-down of MAPK prevents H/R_A-induced ROS generation. (A) Lanes 1, 2 show western blots of ERK1/2 in normoxic WT cells from 2 independent experiments. SiRNA for ERK1 specifically knocked down ERK1 (lanes 3, 4) while siRNA for ERK2 specifically knocked down ERK2 (lanes 5, 6). Scrambled siRNA did not affect ERK1/2 protein expression (data not shown). GAPDH served as loading control. (B) Cells subjected to transfection medium only demonstrated increased ROS after H/R_A(30 min) (bars 1,2). Transfection with siRNA for ERK1 or ERK2 inhibited the H/R_A-induced increase in ROS (bars 3 or 4 vs. 2). Since hypoxia did not significantly increase ROS (Figure 5A, lane 2), the effect of ERK siRNA on ROS level during hypoxia alone was not tested. *Difference from normoxia group (bar 1), #difference from H/R_A group (bar 2), $p < .05$, $n = 5$–7. (C) Transfection of WT cells with adenoviral vector containing green fluorescence protein (GFP) did not alter H/R_A-induced increase in ROS (bar 3 vs. 1), while transfection with dominant negative JNK1 (dnJNK1) prevented this increase (bar 4 vs. 3). *Difference from GFP-normoxia group (bar 1), #difference from GFP-H/R_A group (bar 3), $p < .05$, $n = 5$–7.

increases phosphorylation of ERK1/2 and JNK1 via an NADPH oxidase-insensitive mechanism. Activation of these MAP kinases, in fact, leads to NADPH oxidase activation, causing a major increase in ROS level during reoxygenation.

We used 3 approaches (NBT, DHR 123, and lucigenin-based assays) to document an increased ROS production after H/R_A (Figures 5 and 7). Although endothelial cells have been reported to contain NOX1, NOX2, NOX4, and NOX5 subunits of

NADPH oxidase [4], our data indicate that NADPH oxidase containing NOX2 (gp91phox) in MMEC was responsible for the H/R_A-induced ROS increase, as H/R_A did not elevate ROS in gp91phox$^{-/-}$ cells (Figure 6A).

Intriguingly, our data disagree with reports that NADPH oxidase-derived ROS is an upstream activator of MAP kinases (i.e., reports based on studies with cells of large blood vessels [10] and other cells [9]). We show that H/R_A-induced ROS increase lagged behind MAPK activation (Figures 1A, B and 5A), while genetic deletion of gp91phox, inhibition of NADPH oxidase (DPI and apocynin), and treatment with antioxidants PEG-SOD and ascorbate did not affect MAPK activation (Figures 2 and 3). Currently, we cannot explain the disagreement. Since ROS- and MAPK-sensitive responses are cell- and/or stimulus-specific [10], it is possible that our microvascular endothelial cells responded differently than vascular cells derived from large blood vessels. In this regard, differences between macro- and microvascular endothelial MAPK responses to hypoxia and cytokines have been observed [15].

To our knowledge, the mechanism of H/R-induced MAPK activation in microvascular EC has not been addressed. Although the present study did not aim to determine this mechanism, some of our results permitted examination of this mechanism. Referring to Figure 1 (lane 2 in A and B), ERK1/2 and JNK1 were not activated at the end of 1 h hypoxia. This correlated with the lack of increase in ROS at this time point (Figure 5A, bar 2). Consistently, the mitochondrial respiration blocker rotenone had no effect on H/R_A-induced MAPK activation (Figure 3). Although hypoxia can transiently activate ERK1/2 [28, 29], our findings agree with reports that hypoxia alone does not affect ERK phosphorylation in bovine artery smooth muscle cells [23] or JNK activation in rat cardiac myocytes [6]. It has been shown that upstream c-Src and PKC signaling could lead to ERK1/2 phosphorylation [4, 30]. However, tyrosine kinase and PKC inhibition did not affect H/R_A-induced MAPK activation in MMEC (Figure 4), suggesting that other mechanisms may be involved in this process. To this end, we found that manipulation of the rate of reoxygenation could affect MAPK activation. Substantial MAPK activation was observed after abrupt reoxygenation (normoxic PO_2 reached within several seconds) but not after slow reoxygenation (normoxic PO_2 reached in 10 min) (Figure 1A and B, lane 4 vs. 7). This activation was not due to a possible shear stress effect [33] associated with replacement of culture medium, since replacing medium only, either in normoxic cells or in hypoxic cells without subsequent reoxygenation, did not cause MAPK phosphorylation (lanes 1 and 10, respectively, Figure 1A and B). Since oxygen availability to MMEC during reoxygenation was the only difference between the H/R_A and H/R_S protocols, we suggest that MAPK activation in these cells was sensitive to oxygen. Recently, elevation of molecular oxygen has been proposed to trigger O_2-sensitive signaling pathways in cardiac fibroblasts, including MAPK signaling [27]. Although the mechanism of oxygen sensing is yet to be clarified, it appears that mitochondrial signals (e.g., coupled electron transport, calcium flux) may be required in this process [6, 28]. Finally, the lack of effect of slow reoxygenation on MAPK activation in MMEC did not agree with the reported ERK activation in pulmonary artery EC subjected to slow reoxygenation over 5 min [8]. Presently, we cannot explain this disagreement. It is possible that differences in experimental design as well as differences in behavior between macro- and microvascular EC could account for this disagreement. Because the rate of reoxygenation after hypoxia could play a critical role in the development of tissue injury (e.g., during cardiopulmonary bypass reoxygenation following hypoxia in arrested heart, 14), further work is required to elucidate these differences, including the intriguing possibility that rapid MAPK responses to H/R in the microvascular endothelium (Figure 1) are oxygen-sensitive.

Our data indicate that H/R_A-initiated NADPH oxidase activation and ROS production in MMEC are MAPK-dependent. Pharmacological, siRNA and adenovirus-based inhibition of MEK/ERK and JNK prevented H/R_A-stimulated ROS production and NADPH oxidase activity (Figures 7 and 8). These findings agree with reports that MAPK inhibition prevents both hypoxia-induced NADPH oxidase activation in porcine aortic EC [28] and hyperoxia-induced NADPH oxidase activation and ROS production in human lung EC [24]. Our findings are also consistent with reported (i) ERK1/2-dependent phosphorylation of p47phox subunit of NADPH oxidase, in fMLP-stimulated human blood neutrophils [5], and (ii) ERK1/2-dependent translocation of p47phox from cytosol to membrane in similarly stimulated rat peritoneal neutrophils [31]. Further, ERK1/2 was shown to be involved in $PGF_{2\alpha}$-induced NOX1 protein expression in rat vascular smooth muscle cells [7]. Thus, based on the pivotal roles of p47phox and gp91phox in ROS production in MMEC (Figure 6),

it is possible that H/R_A-induced ERK1/2 and JNK1 activation could also yield p47phox phosphorylation and subsequent NADPH oxidase activation in MMEC. However, elucidation of the mechanism of MAPK-dependent increase in NADPH oxidase activity and the involvement in p47phox in this increased activity were beyond the scope of the present study.

Besides NADPH oxidase-dependent ROS production, H/R_A could result in other rapid MAPK-sensitive cellular responses. We recently showed that H/R_A caused ERK1/2-dependent reduction in interendothelial electrical coupling within 4 min after reoxygenation [26]. ERK1/2 activation was reported to serine-phosphorylate the gap junction protein Cx43, leading to reduced gap junctional conductance and intercellular coupling [37]. Since gap junctional coupling within the vascular wall participates in vasoreactivity [11] and in coordination of microvascular blood flow control [19], rapid MAPK-dependent reduction in coupling, as well as MAPK-sensitive modulation of resistance vessels' tone [17, 32], could affect the minute-to-minute regulation of blood flow in a given organ, including regulation during reperfusion after ischemia and the attendant oxygen delivery.

In conclusion, we show that abrupt, but not slow reoxygenation rapidly activates ERK1/2 and JNK1 in mouse microvascular endothelial cells via a tyrosine kinase-, PKC- and NADPH oxidase-insensitive mechanism, leading to increased NADPH oxidase-dependent ROS production. Since it is possible that the rapid MAPK activation is O_2-sensitive, the present study points to the importance of microvascular endothelial function during reoxygenation and its role in the development of pathophysiology after H/R.

REFERENCES

1. Bain J, McLauchlan H, Elliott M, Cohen P. (2003). The specificities of protein kinase inhibitors: an update. *Biochem J* 371:199–204.
2. Bolon ML, Ouellette Y, Li F, Tyml K. (2005). Abrupt reoxygenation following hypoxia reduces electrical coupling between endothelial cells of wild-type but not connexin40 null mice in oxidant- and PKA-dependent manner. *FASEB J* 19:1725–1727.
3. Brecht S, Kirchhof R, Chromik A, Willesen M, Nicolaus T, Raivich G, Wessig J, Waetzig V, Goetz M, Claussen M, Pearse D, Kuan CY, Vaudano E, Behrens A, Wagner E, Flavell RA, Davis RJ, Herdegen T. (2005). Specific pathophysiological functions of JNK isoforms in the brain. *Eur J Neurosci* 21:363–377.
4. Cai H, Griendling KK, Harrison DG. (2003). The vascular NAD(P)H oxidases as therapeutic targets in cardiovascular diseases. *Trends Pharmacol Sci* 24:471–478.
5. Dewas C, Fay M, Gougerot-Pocidalo MA, El-Benna J. (2000). The mitogen-activated protein kinase extracellular signal-regulated kinase 1/2 pathway is involved in formyl-methionyl-leucyl-phenylalanine-induced p47phox phosphorylation in human neutrophils. *J Immunol* 165:5238–5244.
6. Dougherty CJ, Kubasiak LA, Frazier DP, Li H, Xiong WC, Bishopric NH, Webster KA. (2004). Mitochondrial signals initiate the activation of c-Jun N-terminal kinase (JNK) by hypoxia-reoxygenation. *FASEB J* 18:1060–1070.
7. Fan C, Katsuyama M, Nishinaka T, Yabe-Nishimura C. (2005). Transactivation of the EGF receptor and a PI3 kinase-ATF-1 pathway is involved in the up-regulation of NOX1, a catalytic subunit of NADPH oxidase. *FEBS Lett* 579:1301–1305.
8. Farivar AS, Kinnon-Patterson BC, Barnes AD, McCourtie AS, Mulligan MS. (2005) Cyclosporine modulates the response to hypoxia-reoxygenation in pulmonary artery endothelial cells. *Ann Thorac Surg* 79:1010–1016.
9. Gorin Y, Ricono JM, Wagner B, Kim NH, Bhandari B, Choudhury GG, Abboud HE. (2004). Angiotensin II-induced ERK1/ERK2 activation and protein synthesis are redox-dependent in glomerular mesangial cells. *Biochem J* 381:231–239.
10. Griendling KK, Sorescu D, Lassegue B, Ushio-Fukai M. (2000). Modulation of protein kinase activity and gene expression by reactive oxygen species and their role in vascular physiology and pathophysiology. *Arterioscler Thromb Vasc Biol* 20:2175–2183.
11. Griffith TM. (2004). Endothelium-dependent smooth muscle hyperpolarization: do gap junctions provide a unifying hypothesis? *Br J Pharmacol* 141:881–903.
12. Hansen PR. (1998). Inflammatory alterations in the myocardial microcirculation. *J Mol Cell Cardiol* 30:2555–2559.
13. Hashimoto Y, Itoh K, Nishida K, Okano T, Miyazawa Y, Okinaga K. (1994). Rapid superoxide production by endothelial cells and their injury upon reperfusion. *J Surg Res* 57:693–697.
14. Ihnken K, Morita K, Buckberg GD, Winkelmann B, Beyersdorf F, Sherman MP. (1996). Reduced oxygen tension during cardiopulmonary bypass limits myocardial damage in acute hypoxic immature piglet hearts. *Eur J Cardiothorac Surg* 10:1127–1134.
15. Irwin DC, Tissot van Patot MC, Tucker A, Bowen R. (2005). Direct ANP inhibition of hypoxia-induced inflammatory pathways in pulmonary microvascular and macrovascular endothelial monolayers. *Am J Physiol Lung Cell Mol Physiol* 288:L849–L859.
16. Jerome SN, Kong L, Korthuis RJ. (1994). Microvascular dysfunction in postischemic skeletal muscle. *J Invest Surg* 7:3–16.

17. Khan TA, Bianchi C, Ruel M, Voisine P, Li J, Liddicoat JR, Sellke FW. (2003). Mitogen-activated protein kinase inhibition and cardioplegia-cardiopulmonary bypass reduce coronary myogenic tone. *Circulation* 108 (Suppl 1):II348–II353.
18. Korthuis RJ, Smith JK, Carden DL. (1989). Hypoxic reperfusion attenuates postischemic microvascular injury. *Am J Physiol* 256:H315–H319.
19. Kurjiaka DT, Segal SS. (1995). Conducted vasodilation elevates flow in arteriole networks of hamster striated muscle. *Am J Physiol* 269:H1723–H1728.
20. Li C, Jackson RM. (2002). Reactive species mechanisms of cellular hypoxia-reoxygenation injury. *Am J Physiol Cell Physiol* 282:C227–C241.
21. Lidington D, Ouellette Y, Tyml K. (2000). Endotoxin increases intercellular resistance in microvascular endothelial cells by a tyrosine kinase pathway. *J Cell Physiol* 185:117–125.
22. Mohazzab H, Kaminski PM, Wolin MS. (1997). Lactate and PO_2 modulate superoxide anion production in bovine cardiac myocytes: potential role of NADH oxidase. *Circulation* 96:614–620.
23. Oeckler RA, Arcuino E, Ahmad M, Olson SC, Wolin MS. (2005). Cytosolic NADH redox and thiol oxidation regulate pulmonary arterial force through ERK MAP kinase. *Am J Physiol Lung Cell Mol Physiol* 288:L1017–L1025.
24. Parinandi NL, Kleinberg MA, Usatyuk PV, Cummings RJ, Pennathur A, Cardounel AJ, Zweier JL, Garcia JG, Natarajan V. (2003). Hyperoxia-induced NAD(P)H oxidase activation and regulation by MAP kinases in human lung endothelial cells. *Am J Physiol Lung Cell Mol Physiol* 284:L26–L38.
25. Piacentini L, Karliner JS. (1999). Altered gene expression during hypoxia and reoxygenation of the heart. *Pharmacol Ther* 83:21–37.
26. Rose K, Ouellette Y, Bolon M, Tyml K. (2005). Hypoxia/reoxygenation reduces microvascular endothelial cell coupling by a tyrosine and MAP kinase dependent pathway. *J Cell Physiol* 204:131–138.
27. Roy S, Khanna S, Bickerstaff AA, Subramanian SV, Atalay M, Bierl M, Pendyala S, Levy D, Sharma N, Venojarvi M, Strauch A, Orosz CG, Sen CK. (2003). Oxygen sensing by primary cardiac fibroblasts: a key role of p21(Waf1/Cip1/Sdi1). *Circ Res* 92:264–271.
28. Schafer M, Schafer C, Ewald N, Piper HM, Noll T. (2003). Role of redox signaling in the autonomous proliferative response of endothelial cells to hypoxia. *Circ Res* 92:1010–1015.
29. Seko Y, Tobe K, Ueki K, Kadowaki T, Yazaki Y. (1996). Hypoxia and hypoxia/reoxygenation activate Raf-1, mitogen-activated protein kinase kinase, mitogen-activated protein kinases, and S6 kinase in cultured rat cardiac myocytes. *Circ Res* 78:82–90.
30. Tao Q, Spring SC, Terman BI. (2005). Comparison of the signaling mechanisms by which VEGF, H2O2, and phosphatase inhibitors activate endothelial cell ERK1/2 MAP-kinase. *Microvasc Res* 69:36–44.
31. Waki K, Inanami O, Yamamori T, Kuwabara M. (2003). Extracellular signal-regulated kinase 1/2 is involved in the activation of NADPH oxidase induced by FMLP receptor but not by complement receptor 3 in rat neutrophils. *Free Radic Res* 37:665–671.
32. Wesselman JP, Dobrian AD, Schriver SD, Prewitt RL. (2001). Src tyrosine kinases and extracellular signal-regulated kinase 1/2 mitogen-activated protein kinases mediate pressure-induced c-fos expression in cannulated rat mesenteric small arteries. *Hypertension* 37:955–960.
33. White CR, Stevens HY, Haidekker M, Frangos JA. (2005). Temporal gradients in shear, but not spatial gradients, stimulate ERK1/2 activation in human endothelial cells. *Am J Physiol Heart Circ Physiol* 289:H2350–H2355.
34. Wilson JX, Dixon SJ, Yu J, Nees S, Tyml K. (1996). Ascorbate uptake by microvascular endothelial cells of rat skeletal muscle. *Microcirculation* 3:211–221.
35. Wu F, Tyml K, Wilson JX. (2002). Ascorbate inhibits iNOS expression in endotoxin- and IFN gamma-stimulated rat skeletal muscle endothelial cells. *FEBS Lett* 520:122–126.
36. Yamakoshi Y, Umezawa N, Ryu A, Arakane K, Miyata N, Goda Y, Masumizu T, Nagano T. (2003). Active oxygen species generated from photoexcited fullerene (C60) as potential medicines: O_2* versus $^1O_2$. *J Am Chem Soc* 125:12803–12809.
37. Zhou L, Kasparek EM, Nicholson BJ. (1999). Dissection of the molecular basis of pp60(v-src) induced gating of connexin 43 gap junction channels. *J Cell Biol* 144:1033–1045.